ACS Catalysis

Letter

Cite This: ACS Catal. 2018, 8, 9537–9542

pubs.acs.org/acscatalysis

Cu-Catalyzed Decarboxylative Borylation

Jie Wang,[‡,†] Ming Shang,[‡,†] Helena Lundberg,[‡] Karla S. Feu,[‡] Scott J. Hecker,[§] Tian Qin,[‡] Donna G. Blackmond,[*,‡] and Phil S. Baran[*,‡]

[‡]Department of Chemistry, The Scripps Research Institute (TSRI), North Torrey Pines Road, La Jolla, California 92037, United States

[§]The Medicines Company, 3013 Science Park Road, San Diego, California 92121, United States

Supporting Information

ABSTRACT: A simple method for the conversion of carboxylic acids to boronic esters via redox-active esters (RAEs) is reported using copper catalysis. The scope of this transformation is broad, and compared with the known protocols available, it represents the most inexpensive, rapid, and operationally simple option. In addition to a full exploration of the scope, a kinetic study was performed to elucidate substrate and reagent concentration dependences.

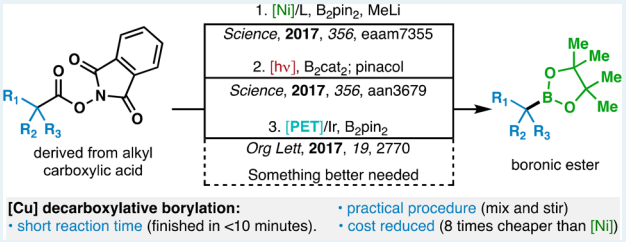

KEYWORDS: *copper catalysis, decarboxylative borylation, redox-active esters, practical protocol, kinetic studies*

The metamorphosis of alkyl carboxylic acids into boronic acids is a powerful transformation that provides a rapid gateway into useful chemical space.[1] In 2017, our lab reported a straightforward method to achieve this through the intermediacy of redox-active esters (RAEs), an inexpensive Ni-catalyst, and an in situ derived boron ate complex (from B_2pin_2).[2] Shortly thereafter, two separate reports emerged from the Aggarwal[3] and Li[4] groups on photochemical and photoinduced electron transfer (PET)-based approaches to the same transformation.[5] Both methods employed RAEs and either a photoactive boron-donor (B_2cat_2) in the case of the former method, or an Ir-based photocatalyst and B_2pin_2 as the boron donor in the latter. These three complementary approaches[6] are clearly of use on a preparative scale, but for process applications, they all suffer certain drawbacks, such as the use of excess/expensive boron donors, low concentrations, or oxygen sensitivity. In addition, certain regions of the world prefer to avoid the use of homogeneous Ni catalysis on scale,[7] or expensive photocatalysts and continuous flow apparatus which add additional cost and engineering considerations. These pragmatic constraints were brought to our attention in the context of the recently approved β-lactamase inhibitor vaborbactam (**1**, Figure 1A, one of two active ingredients in Vabomere).[8] The chiral ester **2** previously served as a key intermediate en route to **1** and was assembled using standard polar transformations in a four-step sequence and required the use of toxic acrolein, as well as kinetic resolution step, resulting in a 50% loss of material.[9] In contrast, a radical disconnection enabled the use of carboxylic acid **4** (prepared in three steps[10]) directly to access **2** in 48% isolated yield. In considering options for the commercial scale-up of this step, the drawbacks of the known decarboxylative borylation (as mentioned above)

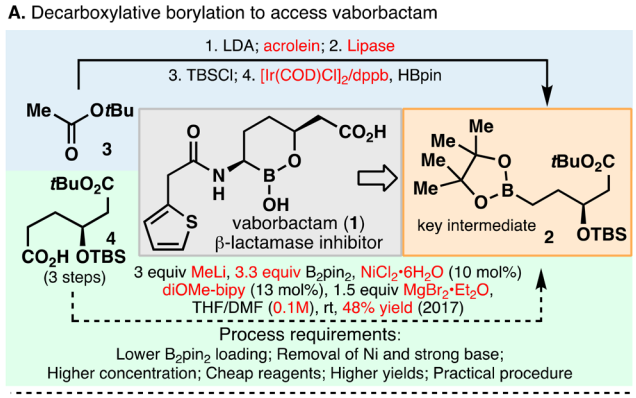

B. Discovery of a Cu-catalyzed decarboxylative borylation

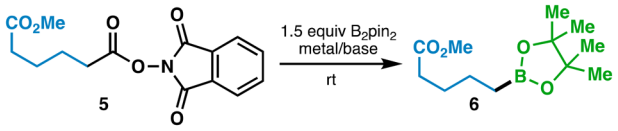

entry	selected optimization conditions	yield (%)[b]
1	$NiCl_2•6H_2O$ (0.1), **L1** (0.13), MeLi (1.5), $MgBr_2•Et_2O$ (1.5)	43
2	$MnBr_2$ (0.05), TMEDA (0.2), EtMgBr (1.5), DME	6
3	CuI (0.1), **L2** (0.1), *t*BuOLi (1.5), $MgBr_2•Et_2O$ (0.2), THF	11
4	$Cu(OAc)_2$ (0.1), **L2** (0.1), *t*BuOLi (1.5), dioxane/DMF	25
5	$Cu(OAc)_2$ (0.1), **L2** (0.1), $LiOH•H_2O$ (4), $MgBr_2•Et_2O$ (0.2)	48
6	$Cu(acac)_2$ (0.2), $LiOH•H_2O$ (10), $MgBr_2•Et_2O$ (0.8), dioxane/DMF	62
7	$Cu(acac)_2$ (0.2), $LiOH•H_2O$ (15), $MgCl_2$ (1.5), dioxane/DMF	69
8	the same as entry 7 with $Cu(acac)_2$ (0.3), B_2pin_2 (3)	86

Figure 1. (A) Decarboxylative borylation to access vaborbactam. (B) Discovery of a Cu-catalyzed decarboxylative borylation and optimization of reaction conditions. B_2pin_2 = bis(pinacolato)diboron, TMEDA = *N,N,N′,N′*-tetramethylethylenediamine.

Received: July 25, 2018
Revised: September 7, 2018
Published: September 13, 2018

DOI: 10.1021/acscatal.8b02928
ACS Catal. 2018, 8, 9537–9542

Scheme 1. Scope of the Cu-Catalyzed Decarboxylative Borylation with NHPI Redox-Active Esters[g]

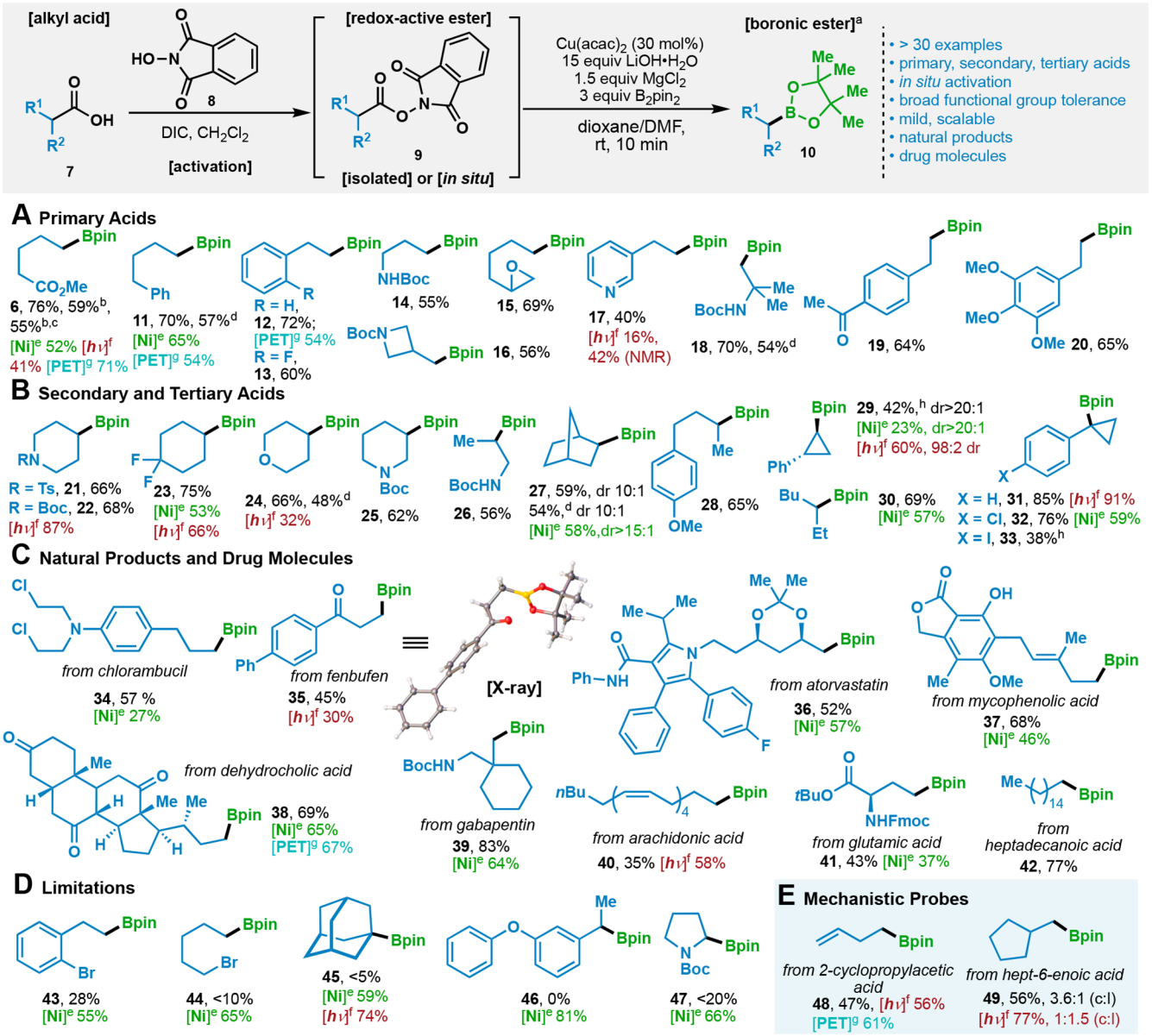

[g]Reaction conditions: (a) RAE (1.0 equiv), $Cu(acac)_2$ (30 mol %), $LiOH·H_2O$ (15.0 equiv), $MgCl_2$ (1.5 equiv), B_2pin_2 (3.0 equiv), dioxane/DMF, rt, 10 min. (b) $Cu(acac)_2$ (20 mol %) and B_2pin_2 (1.5 equiv) were used. (c) 3.5 mmol scale. (d) In situ reaction with NHPI (1.0 equiv) and DIC (1.0 equiv). (e) [**Ni**] yield referred to reported yield in ref 2. (f) [***hν***] yield referred to reported yield in ref 3. (g) [**PET**] yield referred to reported yield in ref 4. (h) solvent MTBE/DMF was used. Ts = tosyl, Boc = *tert*-butyloxycarbonyl, Fmoc = fluorenylmethyloxycarbonyl. NHPI = *N*-hydroxyphthalimide, DIC = *N,N'*-diisopropylcarbodiimide.

were magnified. Here we report a new protocol to achieve this transformation featuring a simple procedure, short reaction times (0.1 h), and a catalyst system based on inexpensive Cu without the need for external ligands. The cost associated with the scale up of this process is roughly an order of magnitude less than its Ni-catalyzed counterpart. The kinetics of this intriguing transformation have also been studied in depth.

The development of Cu-catalyzed decarboxylative borylation was guided by industrial feedback regarding the minimization of B_2pin_2 employed, as this was not only a cost driver but also difficult to remove from the product. Thus, this reagent was limited to 1.5 equiv for all explorations on the conversion of model RAE **5** to boronic ester **6** (Figure 1B, see the Supporting Information for an exhaustive list of conditions evaluated). As shown in entry 1, standard Ni-catalyzed conditions with this reduced B_2pin_2 loading resulted in 43% yield of **6**. A promising hit was obtained by employing conditions reported by the Cook lab for Mn-catalyzed borylation of alkyl halides (6%, entry 2).[11] Oestreich's decarboxylative silylation using Cu catalysis inspired the conditions attempted in entry 3 (11%).[12] Systematic screening of Cu sources, solvents, and ligands led to a gradual increase in yield (entry 4).[13] The use of an old bottle of *t*BuOLi led to the realization that LiOH was actually the active base for our reaction and the first promising yields were observed when used in excess (entry 5). Subsequent ligand screening unveiled that no external ligand was actually needed (entry 6) and additional evaluation of both the Mg source and Cu catalyst

DOI: 10.1021/acscatal.8b02928
ACS Catal. 2018, 8, 9537–9542

Scheme 2. Cu-Catalyzed Decarboxylative Borylation to Synthesize Target Compound 2 and Cost Comparisons with Other Methods[||]

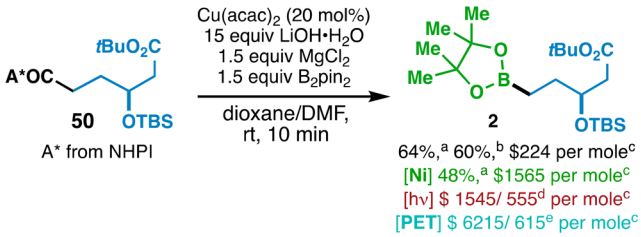

[||](a) 0.1 mmol scale. (b) 2.5 mmol scale. (c) The cost of raw materials for one mole reaction setup. See the Supporting Information for details. (d) B_2cat_2 prepared from $B_2(NMe_2)_4$ and catechol. e) $Ir[(ppy)_2dtbpy]PF_6$ prepared from $IrCl_3 \times H_2O$ in 2 steps.

led to optimized conditions shown in entry 7 (69% yield). If the loading of B_2pin_2 and Cu were increased, the yield could be further increased to 86% (entry 8). The experimental simplicity of this new protocol is worthy of additional comment. All components are simply added to a flask, the air is purged and replaced with inert gas, followed by addition of solvent—the reaction is complete within minutes at ambient temperature.[14]

With an optimized protocol in hand, the scope of this Cu-catalyzed borylation methodology was explored (Scheme 1). To test the generality of this protocol, 3.0 equiv of B_2pin_2 and 30 mol % of $Cu(acac)_2$ was used for the small-scale preparation of substrates in Scheme 1. Under standard conditions, a variety of primary and secondary RAE substrates were converted to their Bpin derivatives smoothly (Scheme 1A,B). Simple cyclic (**21**−**25**, **27**, and **29**) and acyclic (**6**, **11**−**20**, **26**, **28**, and **30**) boronic esters are easily accessed in higher or comparable yield to known decarboxylative borylation methods (comparative yields are shown for Ni[2], *hν*[3] and PET[4]-based conditions where available). Scalability of this reaction was demonstrated through the preparation of **6** on 3.5 mmol scale with 1.5 equiv of B_2pin_2 and 20 mol % of $Cu(acac)_2$. An in situ protocol from the parent alkyl carboxylic acids was also developed, providing access to several boronic esters (**11**, **18**, **24**, and **27**) in similar yields. RAEs with *β*-nitrogen substitution were tolerated and afforded the *β*-amino boronates (**18**, **25** and **26**), which are difficult to access otherwise. Furthermore, heterocyclic moieties were tolerated under the mild reaction conditions, even in the absence of an external ligand on copper; the 3-pyridyl Bpin ester product (**17**) was formed in moderate yield. Despite the use of $LiOH{\cdot}H_2O$, a variety of functionalities such as esters (**6**), Boc groups (**14**, **16**, **18**, **22**, **25**, and **26**), epoxides (**15**), ketones (**19**), and ethers (**20** and **28**) were intact under the mild conditions, presumably due to the limited solubility of $LiOH{\cdot}H_2O$ in organic solvents. Cyclopropyl-based tertiary RAEs were also found to be suitable substrates for this transformation (**31**−**33**). Although active low-valent Cu species are likely generated during this reaction, aryl chloride (**32**) was left unscathed, while aryl iodide containing substrates (**33**) could be obtained in synthetically useful yield with judicious choice of solvent.

As a testament to the chemoselectivity of the method, complex natural products and drug molecule acid derivatives (**34**−**42**) were further evaluated in this study (Scheme 1C). Thus, diverse scaffolds containing displacement-prone chlorides (**34**), ketones (**35** and **38**), lactones (**37**), acetonides

Scheme 3. (A) Kinetic Studies of Cu-Catalyzed Decarboxylative Borylation and Concentration Dependences for This Transformation; (B) Reactions Orders in [Cu] for Formation of Product and Major Byproduct; (C) Relationship between the Relative Rates of Productive and Side Reactions to mol % Cu[a]

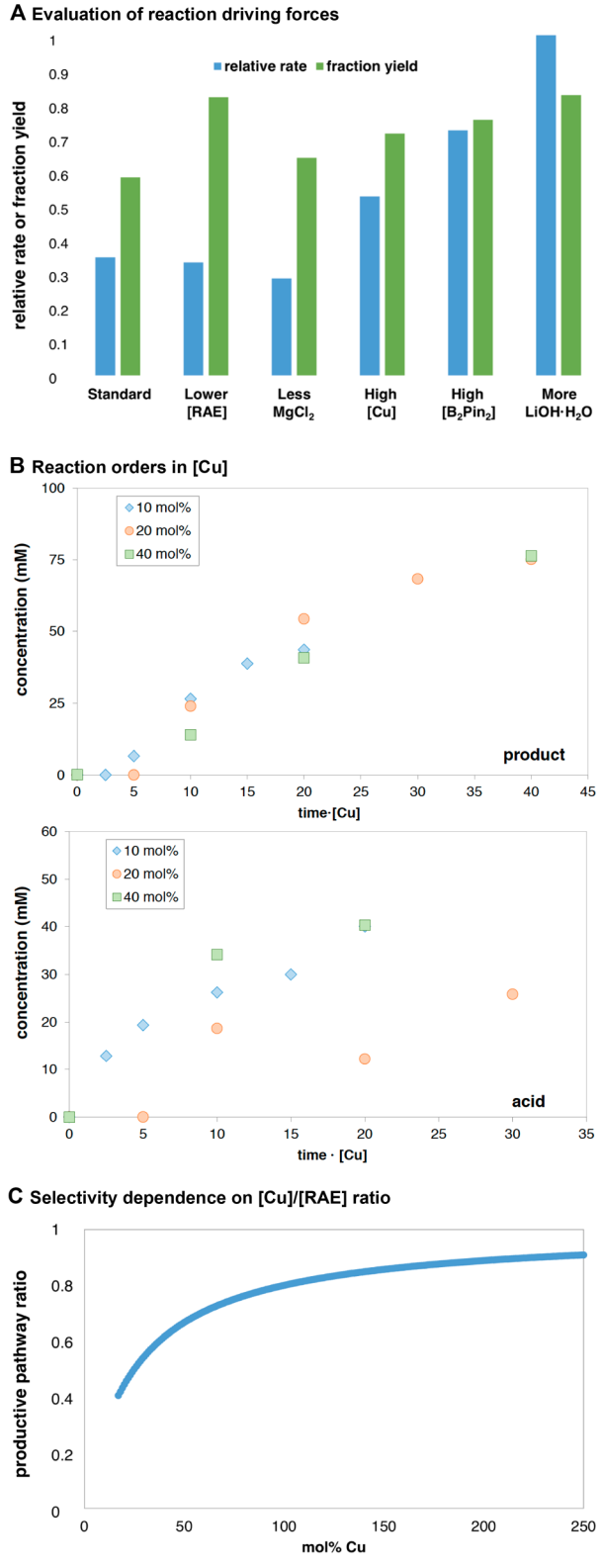

[a]Selectivity to desired product is enhanced by high [Cu] and low [RAE]. Yields were determined by LC-UV.

DOI: 10.1021/acscatal.8b02928
ACS Catal. 2018, 8, 9537−9542

Scheme 4. Proposed Cu-Catalyzed Borylation Mechanism

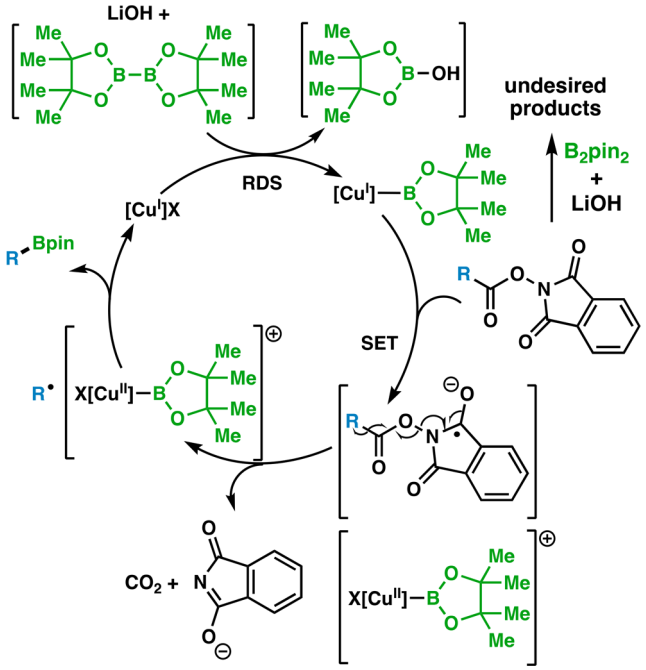

(**36**), base-labile Fmoc groups (**41**) and alkenes (**37** and **40**) were left unperturbed under the reaction conditions. Six of the nine substrates investigated were obtained with an enhanced yield and reduced reaction time when compared to established methods.

Although this protocol was proved to be successful on a range of substrates, there are some limitations. Diminished yields were observed for acids containing aryl (**43**) or alkyl (**44**) bromides due to competitive protodebromination or borylation of bromide. Tertiary (**45**), benzylic (**46**), and α-amino (**47**) substrates are also nonproductive or low-yielding.

Following the substrate scope exploration, a preliminary mechanistic inquiry was conducted (Scheme 1E). Radical clock experiments, including cyclopropyl ring opening (**48**) and *5-exo-trig* radical cyclization (**49**), suggested the presence of alkyl radicals during this protocol, which is consistent with reported RAE decarboxylative coupling studies.[15]

After achieving the process requirements and demonstrating the generality of this Cu-catalyzed decarboxylative borylation, this protocol was ultimately tested on the genuine substrate **50**. Gratifyingly, the desired product **2** was obtained in 64% yield with 1.5 equiv of B_2pin_2 and 20 mol % of $Cu(acac)_2$ (Scheme 2). As a further test of its scalability, boronate **2** was isolated in similar yield during 2.5 mmol scale synthesis, and the reaction was complete in less than 10 min. Not only was a higher yield achieved compared with our previous Ni-catalyzed borylation conditions, but the decreased stoichiometry of B_2pin_2, removal of strong base, and absence of exogenous ligands led to a dramatically less expensive decarboxylative borylation protocol ($224 per mole vs Ni $1565 per mole). This procedure also compares favorably from a cost perspective to the other known decarboxylative borylation methods.[16]

Kinetic studies of the borylation reaction were carried out on RAE derived from 5-phenylvaleric acid to understand the concentration dependences and the role of the reaction components. Following the time course of the reaction under our initial standard conditions (Scheme 1A, entry 8) revealed that the reaction occurs extremely rapidly, with full consumption of the RAE within 3 min of initiating the reaction and 5-phenylvaleric acid forming as the major byproduct (see the Supporting Information for details). The concentration dependences were probed by varying initial concentrations separately for each component and comparing reaction rate to that under standard conditions. Parameters for increased rate include increased $[B_2pin_2]$, $[Cu(acac)_2]$, and equivalents of $LiOH{\cdot}H_2O$, whereas reaction rate was not significantly influenced by changes in equivalents of $MgCl_2$ or [RAE] (Scheme 3A). Interestingly, the fraction yield increased substantially in reactions run at *lower* [RAE] from 60% to 85%, indicating that under these conditions, a larger percentage of the RAE is directed toward the productive reaction pathway. This suggests that while the productive reaction exhibits zero order kinetics in [RAE], unproductive side reactions have a positive dependence on RAE concentration.

We examined the role of each component in turn by removing them one at a time and probing the effect on both product yield and consumption of RAE (see the Supporting Information for details). It was found that a Cu(I) source does not significantly reduce product yield from that observed with the Cu(II) source used under standard conditions. Reactions carried out with either source of Cu removed from the reaction mixture afforded no product, but did consume RAE.

Removal of $MgCl_2$ also resulted in no product formation, although RAE was consumed, albeit more slowly than under standard reaction conditions. Interestingly, removal of either $LiOH{\cdot}H_2O$ or B_2pin_2 completely suppressed the consumption of RAE, suggesting a role for both species in activating the catalyst for product turnover as well as for side reactions of RAE.

Further examination of the role of $[Cu(acac)_2]$ in both productive and unproductive reactions is shown in Scheme 3B, where the concentration of product **11** and the major byproduct 5-phenylvaleric acid is plotted as a function of (time·[Cu]) according to the methodology of Burés.[17] Overlay for reactions at different [Cu] in Scheme 3B (top) indicates first order kinetics in [Cu] for the borylation reaction, while the lack of overlay for acid formation in the plot of Scheme 3B (bottom) suggests that the consumption of RAE in unproductive side reactions are not a simple function of the concentration of Cu. These results suggest the rate laws shown in equations 1 and 2 that describe the formation of the borylation product and the overall consumption of RAE, respectively. The productive Cu-catalyzed reaction may be maximized at the expense of the Cu-free byproduct formation by maximizing the ratio given in eq 3. Employing dilute conditions of [RAE] and/or high catalyst loadings thus offers a practical means of increasing reaction efficiency. The selectivity dependence on the [RAE]/[Cu] ratio is illustrated in the model in Scheme 3C,[18] where the ratio of $k'/k = 0.25$ is derived from the data in Scheme 3B.

$$\frac{\mathrm{d[product]}}{\mathrm{d}t} = k{\cdot}[B_2pin_2]{\cdot}[LiOH{\cdot}H_2O]{\cdot}[Cu] \quad (1)$$

$$-\frac{\mathrm{d[RAE]}}{\mathrm{d}t} = [B_2pin_2]{\cdot}[LiOH{\cdot}H_2O](k{\cdot}[Cu] + k'{\cdot}[RAE]) \quad (2)$$

DOI: 10.1021/acscatal.8b02928
ACS Catal. 2018, 8, 9537−9542

$$\frac{d[product]}{d[RAE]} = \frac{k\cdot[Cu]}{k\cdot[Cu] + k'\cdot[RAE]} \quad (3)$$

These results suggest the mechanistic picture shown in Scheme 4. The observed positive order kinetics in [LiOH·H_2O] and [B_2pin_2] may be rationalized by rate-determining formation of a complex with Cu. This complex may then react with the RAE forming a radical complex that fragments to release CO_2 and phthalimide.[19] Finally, radical recombination will result in the borylated alkyl product and thus close the productive catalytic cycle. The formation of side products from the RAE is noncatalyzed and occur in the presence of B_2pin_2 and LiOH·H_2O.

This work constitutes another example of the use of Cu-catalysis for inducing decarboxylation of redox-active esters.[12,20] In the present case, inexpensive and rapid access to boronic esters combined with a clear analysis of concentration dependences may facilitate large-scale adoption. The simple experimental protocol described herein might inspire other radical-based cross couplings and functional group interconversions using Cu.

■ ASSOCIATED CONTENT

Supporting Information

The Supporting Information is available free of charge on the ACS Publications website at DOI: 10.1021/acscatal.8b02928.

Experimental procedures, detailed optimization, and full spectroscopic data for compounds of ^1H and ^{13}C NMR spectra (PDF)

■ AUTHOR INFORMATION

Corresponding Authors

*E-mail: blackmon@scripps.edu.
*E-mail: pbaran@scripps.edu.

ORCID

Ming Shang: 0000-0002-0785-8427
Phil S. Baran: 0000-0001-9193-9053

Author Contributions

†These authors contributed equally.

Notes

The authors declare no competing financial interest.

■ ACKNOWLEDGMENTS

Financial support for this work was provided by NIH (grant number GM-118176). The Swedish Research Council, The Foundation Blanceflor Boncompagni-Ludovisi née Bildt, Stiftelsen Olle Engkvist Byggmästare, and The Hans Werthén Fund Scholarship supported research fellowships to H.L; Zhejiang Yuanhong Medicine Technology Co. Ltd. supported fellowships to M.S.; São Paulo Research Foundation (FAPESP, 2017/08128-7) supported fellowships to K.S.F. We thank D.-H. Huang and L. Pasternack (The Scripps Research Institute) for assistance with nuclear magnetic resonance spectroscopy. We are grateful to Dr. Jason S. Chen (The Scripps Research Institute) for assistance with the kinetic studies and Michael Collins (Pfizer) for providing atorvastatin sample. We also thank A.L. Rheingold, C.E. Moore and M. Gembicky (University of California, San Diego) for X-ray crystallographic analysis.

■ REFERENCES

(1) (a) Trippier, P. C.; McGuigan, C. Boronic Acids in Medicinal Chemistry: Anticancer, Antibacterial and Antiviral Applications. *MedChemComm* **2010**, *1*, 183−198. (b) Draganov, A.; Wang, D.; Wang, B. The Future of Boron in Medicinal Chemistry: Therapeutic and Diagnostic Applications. In *Atypical Elements in Drug Design*, Schwarz, J., Ed.; Springer, 2014; pp 1−27. (c) Ballatore, C.; Huryn, D. M.; Smith, A. B., 3rd Carboxylic Acid (Bio)Isosteres in Drug Design. *ChemMedChem* **2013**, *8*, 385−395.

(2) Li, C.; Wang, J.; Barton, L. M.; Yu, S.; Tian, M.; Peters, D. S.; Kumar, M.; Yu, A. W.; Johnson, K. A.; Chatterjee, A. K.; Yan, M.; Baran, P. S. Decarboxylative Borylation. *Science* **2017**, *356*, eaam7355.

(3) Fawcett, A.; Pradeilles, J.; Wang, Y.; Mutsuga, T.; Myers, E. L.; Aggarwal, V. K. Photoinduced Decarboxylative Borylation of Carboxylic Acids. *Science* **2017**, *357*, 283−286.

(4) Hu, D.; Wang, L.; Li, P. Decarboxylative Borylation of Aliphatic Esters under Visible-Light Photoredox Conditions. *Org. Lett.* **2017**, *19*, 2770−2773.

(5) Redox-active esters were also employed in sp^2-boronic ester formation, see: (a) Candish, L.; Teders, M.; Glorius, F. Transition-Metal-Free, Visible-Light-Enabled Decarboxylative Borylation of Aryl N-Hydroxyphthalimide Esters. *J. Am. Chem. Soc.* **2017**, *139*, 7440−7443. (b) Cheng, W.-M.; Shang, R.; Zhao, B.; Xing, W.-L.; Fu, Y. Isonicotinate Ester Catalyzed Decarboxylative Borylation of (Hetero)-Aryl and Alkenyl Carboxylic Acids through N-Hydroxyphthalimide Esters. *Org. Lett.* **2017**, *19*, 4291−4294.

(6) For review on decarboxylative borylation, see: Xu, L. Decarboxylative Borylation: New Avenues for the Preparation of Organoboron Compounds. *Eur. J. Org. Chem.* **2018**, *2018*, 3884−3890.

(7) (a) Cameron, K. S.; Buchner, C.; Tchounwou, P. B. Exploring the Molecular Mechanisms of Nickel-Induced Genotoxicity and Carcinogenicity: A Literature Review. *Rev. Environ. Health* **2011**, *26*, 81−92. Risk Assessment (RAC) for Evaluation of Limit Values for Nickel and its Compounds in the Workplace from European Chemical Agency (ECHA), ECHA/RAC/A77-0-0000001412-86-189/F.

(8) FDA news release August 29th, 2017. https://www.fda.gov/NewsEvents/Newsroom/PressAnnouncements/ucm573955.htm (accessed July 24, 2018).

(9) (a) Hecker, S. J.; Reddy, K. R.; Totrov, M.; Hirst, G. C.; Lomovskaya, O.; Griffith, D. C.; King, P.; Tsivkovski, R.; Sun, D.; Sabet, M.; Tarazi, Z.; Clifton, M. C.; Atkins, K.; Raymond, A.; Potts, K. T.; Abendroth, J.; Boyer, S. H.; Loutit, J. S.; Morgan, E. E.; Durso, S.; Dudley, M. N. Discovery of A Cyclic Boronic Acid β-Lactamase Inhibitor (RPX7009) with Utility vs Class A Serine Carbapenemases. *J. Med. Chem.* **2015**, *58*, 3682−3692. (b) Vrielynck, S.; Vandewalle, M.; Garcia, A. M.; Mascareñas, K. L.; Mouriño, A. A. A Chemoenzymatic Synthesis of α-Ring Key-Intermediates for 1α,25-Dihydroxyvitamin D_3 and Analogues. *Tetrahedron Lett.* **1995**, *36*, 9023−9026.

(10) Ghosh, M.; Miller, M. J. Synthesis of A Bicyclic Oxamazin. A Novel Heteroatom Activated β-Lactam. *Tetrahedron* **1996**, *52*, 4225−4238.

(11) (a) Atack, T. C.; Cook, S. P. Manganese-Catalyzed Borylation of Unactivated Alkyl Chlorides. *J. Am. Chem. Soc.* **2016**, *138*, 6139−6142. (b) Atack, T. C.; Lecker, R. M.; Cook, S. P. Iron-Catalyzed Borylation of Alkyl Electrophiles. *J. Am. Chem. Soc.* **2014**, *136*, 9521−9523.

(12) Xue, W.; Oestreich, M. Copper-Catalyzed Decarboxylative Radical Silylation of Redox-Active Aliphatic Carboxylic Acid Derivatives. *Angew. Chem., Int. Ed.* **2017**, *56*, 11649−11652.

(13) (a) Yang, C.-T.; Zhang, Z.-Q.; Tajuddin, H.; Wu, C.-C.; Liang, J.; Liu, J.-H.; Fu, Y.; Czyzewska, M.; Steel, P. G.; Marder, T. B.; Liu, L. Alkylboronic Esters from Copper-Catalyzed Borylation of Primary and Secondary Alkyl Halides and Pseudohalides. *Angew. Chem., Int. Ed.* **2012**, *51*, 528−532. (b) Ito, H.; Kubota, K. Copper(I)-Catalyzed Boryl Substitution of Unactivated Alkyl Halides. *Org. Lett.* **2012**, *14*, 890−893. (c) Kubota, K.; Yamamoto, E.; Ito, H. Copper(I)-

DOI: 10.1021/acscatal.8b02928
ACS Catal. 2018, 8, 9537−9542

Catalyzed Borylative *exo*-Cyclization of Alkenyl Halides Containing Unactivated Double Bond. *J. Am. Chem. Soc.* **2013**, *135*, 2635−2640. (d) Zhang, Z.-Q.; Yang, C.-T.; Liang, L.-J.; Xiao, B.; Lu, X.; Liu, J.-H.; Sun, Y.-Y.; Marder, T. B.; Fu, Y. Copper-Catalyzed/Promoted Cross-Coupling of Gem-Diborylalkanes with Nonactivated Primary Alkyl Halides: An Alternative Route to Alkylboronic Esters. *Org. Lett.* **2014**, *16*, 6342−6345. (e) Bose, S. K.; Brand, S.; Omoregie, H. O.; Haehnel, M.; Maier, J.; Bringmann, G.; Marder, T. B. Highly Efficient Synthesis of Alkylboronate Esters via Cu(II)-Catalyzed Borylation of Unactivated Alkyl Bromides and Chlorides in Air. *ACS Catal.* **2016**, *6*, 8332−8335. (f) Liu, M.-Y.; Hong, S.-B.; Zhang, W.; Deng, W. Expedient Copper-Catalyzed Borylation Reactions Using Amino Acids as Ligands. *Chin. Chem. Lett.* **2015**, *26*, 373−376. (g) Yoshida, H.; Takemoto, Y.; Kamio, S.; Osaka, I.; Takaki, K. Copper-Catalyzed Direct Borylation of Alkyl, Alkenyl and Aryl Halides with B(dan). *Org. Chem. Front.* **2017**, *4*, 1215−1219. (h) Iwamoto, H.; Akiyama, A.; Hayama, K.; Ito, H. Copper(I)-Catalyzed Stereo- and Chemoselective Borylative Radical Cyclization of Alkyl Halides Bearing an Alkene Moiety. *Org. Lett.* **2017**, *19*, 2614−2617. (i) Su, W.; Gong, T.-J.; Lu, X.; Xu, M.-Y.; Yu, C.-G.; Xu, Z.-Y.; Yu, H.-Z.; Xiao, B.; Fu, Y. Ligand-Controlled Regiodivergent Copper-Catalyzed Alkylboration of Alkenes. *Angew. Chem., Int. Ed.* **2015**, *54*, 12957−12961. (j) Ding, S.; Xu, L.; Li, P. Copper-Catalyzed Boron-Selective $C(sp^2)$-$C(sp^3)$ Oxidative Cross-Coupling of Arylboronic Acids and Alkyltrifluoroborates Involving a Single-Electron Transmetalation Process. *ACS Catal.* **2016**, *6*, 1329−1333.

(14) For graphic procedure, see the Supporting Information for details.

(15) (a) Cornella, J.; Edwards, J. T.; Qin, T.; Kawamura, S.; Wang, J.; Pan, C.-M.; Gianatassio, R.; Schmidt, M.; Eastgate, M. D.; Baran, P. S. Practical Ni-Catalyzed Aryl−Alkyl Cross-Coupling of Secondary Redox-Active Esters. *J. Am. Chem. Soc.* **2016**, *138*, 2174−2177. (b) Qin, T.; Cornella, J.; Li, C.; Malins, L. R.; Edwards, J. T.; Kawamura, S.; Maxwell, B. D.; Eastgate, M. D.; Baran, P. S. A General Alkyl-Alkyl Cross-Coupling Enabled by Redox-Active Esters and Alkylzinc Reagents. *Science* **2016**, *352*, 801−805. (c) Wang, J.; Qin, T.; Chen, T.-G.; Wimmer, L.; Edwards, J. T.; Cornella, J.; Vokits, B.; Shaw, S. A.; Baran, P. S. Nickel-Catalyzed Cross-Coupling of Redox-Active Esters with Boronic Acids. *Angew. Chem., Int. Ed.* **2016**, *55*, 9676−9679. (d) Toriyama, F.; Cornella, J.; Wimmer, L.; Chen, T.-G.; Dixon, D. D.; Creech, G.; Baran, P. S. Redox-Active Esters in Fe-Catalyzed C−C Coupling. *J. Am. Chem. Soc.* **2016**, *138*, 11132−11135. (e) Qin, T.; Malins, L. R.; Edwards, J. T.; Merchant, R. R.; Novak, A. J. E.; Zhong, J. Z.; Mills, R. B.; Yan, M.; Yuan, C.; Eastgate, M. D.; Baran, P. S. Nickel-Catalyzed Barton Decarboxylation and Giese Reactions: A Practical Take on Classic Transforms. *Angew. Chem., Int. Ed.* **2017**, *56*, 260−265. (f) Sandfort, F.; O'Neill, M. J.; Cornella, J.; Wimmer, L.; Baran, P. S. Alkyl−(Hetero)Aryl Bond Formation via Decarboxylative Cross-Coupling: A Systematic Analysis. *Angew. Chem., Int. Ed.* **2017**, *56*, 3319−3323. (g) Edwards, J. T.; Merchant, R. R.; McClymont, K. S.; Knouse, K. W.; Qin, T.; Malins, L. R.; Vokits, B.; Shaw, S. A.; Bao, D.-H.; Wei, F.-L.; Zhou, T.; Eastgate, M. D.; Baran, P. S. Decarboyxlative Alkenylation. *Nature* **2017**, *545*, 213−218. (h) Smith, J.; Qin, T.; Merchant, R. R.; Edwards, J. T.; Malins, L. R.; Liu, Z.; Che, G.; Shen, Z.; Shaw, S. A.; Eastgate, M. D.; Baran, P. S. Decarboxylative Alkynylation. *Angew. Chem., Int. Ed.* **2017**, *56*, 11906−11910. (i) For another example of using RAE cross-coupling, see: Huihui, K. M. M.; Caputo, J. A.; Melchor, Z.; Olivares, A. M.; Spiewak, A. M.; Johnson, K. A.; DiBenedetto, T. A.; Kim, S.; Ackerman, L. K. G.; Weix, D. A. Decarboxylative Cross-Electrophile Coupling of N-Hydroxyphthalimide Esters with Aryl Iodides. *J. Am. Chem. Soc.* **2016**, *138*, 5016−5019. (j) For a seminal use of RAEs of the phthalimide-type, see: Okada, K.; Okamoto, K.; Oda, M. A New and Practical Method of Decarboxylation: Photosensitized Decarboxylation of N-Acyloxyphthalimides via Electron-Transfer Mechanism. *J. Am. Chem. Soc.* **1988**, *110*, 8736−8738.

(16) For rough cost calculation, see the Supporting Information for details.

(17) Burés, J. A Simple Graphical Method to Determine the Order in Catalyst. *Angew. Chem., Int. Ed.* **2016**, *55*, 2028−2031.

(18) See the Supporting Information for equations derived from eq 3.

(19) SET reduction of RAEs by Cu(I) species has previously been suggested, see refs 12,20.

(20) (a) Zhao, W.; Wurz, R. P.; Peters, J. C.; Fu, G. C. Photoinduced, Copper-Catalyzed Decarboxylative C−N coupling to Generate Protected Amines: An Alternative to the Curtius Rearrangement. *J. Am. Chem. Soc.* **2017**, *139*, 12153−12156. (b) Mao, R.; Frey, A.; Balon, J.; Hu, X. Decarboxylative $C(sp^3)$−N Cross-Coupling via Synergetic Photoredox and Copper Catalysis. *Nat. Catal.* **2018**, *1*, 120−126. (c) Mao, R.; Balon, J.; Hu, X. Cross-Coupling of Alkyl Redox-Active Esters with Benzophenone imines: Tandem Photoredox and Copper Catalysis. *Angew. Chem., Int. Ed.* **2018**, *57*, 9501−9504.

DOI: 10.1021/acscatal.8b02928
ACS Catal. 2018, 8, 9537−9542